Focal Gains of *VEGFA* and Molecular Classification of Hepatocellular Carcinoma

Derek Y. Chiang,[1,4] Augusto Villanueva,[6] Yujin Hoshida,[2,4] Judit Peix,[6] Philippa Newell,[6] Beatriz Minguez,[6] Amanda C. LeBlanc,[7,8] Diana J. Donovan,[3] Swan N. Thung,[8] Manel Solé,[10] Victoria Tovar,[10] Clara Alsinet,[10] Alex H. Ramos,[1,4] Jordi Barretina,[1,4] Sasan Roayaie,[9] Myron Schwartz,[9] Samuel Waxman,[7] Jordi Bruix,[10] Vincenzo Mazzaferro,[11] Azra H. Ligon,[3] Vesna Najfeld,[7,8] Scott L. Friedman,[6] William R. Sellers,[5] Matthew Meyerson,[1,4] and Josep M. Llovet[6,10]

[1]Department of Medical Oncology and Center for Cancer Genome Discovery and [2]Department of Pediatric Oncology, Dana-Farber Cancer Institute, [3]Department of Pathology, Brigham and Women's Hospital, Boston, Massachusetts; [4]Cancer Program, Broad Institute of Harvard and MIT, [5]Novartis Institutes for Biomedical Research, Cambridge, Massachusetts; [6]Mount Sinai Liver Cancer Program, Division of Liver Diseases, [7]Division of Hematology/Oncology, Department of Medicine, [8]Department of Pathology, and [9]Division of Surgical Oncology, Department of Surgery, Mount Sinai School of Medicine, New York, New York; [10]Liver Unit, BCLC Group, HCC Translational Research Lab and Department of Pathology, IDIBAPS, CIBERehd, Hospital Clínic, Barcelona, Spain; and [11]Gastrointestinal Surgery and Liver Transplantation Unit, National Cancer Institute, Milan, Italy

Abstract

Hepatocellular carcinomas represent the third leading cause of cancer-related deaths worldwide. The vast majority of cases arise in the context of chronic liver injury due to hepatitis B virus or hepatitis C virus infection. To identify genetic mechanisms of hepatocarcinogenesis, we characterized copy number alterations and gene expression profiles from the same set of tumors associated with hepatitis C virus. Most tumors harbored 1q gain, 8q gain, or 8p loss, with occasional alterations in 13 additional chromosome arms. In addition to amplifications at 11q13 in 6 of 103 tumors, 4 tumors harbored focal gains at 6p21 incorporating *vascular endothelial growth factor A* (*VEGFA*). Fluorescence *in situ* hybridization on an independent validation set of 210 tumors found 6p21 high-level gains in 14 tumors, as well as 2 tumors with 6p21 amplifications. Strikingly, this locus overlapped with copy gains in 4 of 371 lung adenocarcinomas. Overexpression of VEGFA via 6p21 gain in hepatocellular carcinomas suggested a novel, non–cell-autonomous mechanism of oncogene activation. Hierarchical clustering of gene expression among 91 of these tumors identified five classes, including "*CTNNB1*", "proliferation", "IFN-related", a novel class defined by polysomy of chromosome 7, and an unannotated class. These class labels were further supported by molecular data; mutations in *CTNNB1* were enriched in the "*CTNNB1*" class, whereas insulin-like growth factor I receptor and RPS6 phosphorylation were enriched in the "proliferation" class. The enrichment of signaling pathway alterations in gene expression classes provides insights on hepatocellular carcinoma pathogenesis. Furthermore, the prevalence of *VEGFA* high-level gains in multiple tumor types suggests indications for clinical trials of antiangiogenic therapies. [Cancer Res 2008;68(16):6779–88]

Note: Supplementary data for this article are available at Cancer Research Online (http://cancerres.aacrjournals.org/).

Requests for reprints: Josep M. Llovet, Division of Liver Diseases, Mount Sinai School of Medicine, 1425 Madison Avenue, Box 1123, New York, NY 10029. Phone: 212-659-9503; Fax: 212-849-2574; E-mail: Josep.Llovet@mssm.edu or Matthew Meyerson, Department of Medical Oncology, Dana-Farber Cancer Institute, 44 Binney Street, Dana 1537, Boston, MA 02115. E-mail: Matthew_Meyerson@dfci.harvard.edu.

doi:10.1158/0008-5472.CAN-08-0742

Introduction

Hepatocellular carcinoma is the third leading cause of cancer deaths worldwide. These tumors arise in the context of chronic liver injury, inflammation, and hepatocyte proliferation provoked by several etiologies. Hepatitis C virus is the most prevalent etiology in the United States and Europe, whereas hepatitis B virus is endemic in Asia and Africa (1, 2). The critical genomic hits at preneoplastic stages are not well defined, although aberrant methylation, genomic instability, and TERT activation have been reported. In overt hepatocellular carcinoma, deregulated oncogenes (*MET, CTNNB1, MYC*, and *CCND1*) and tumor suppressor genes (*TP53, PTEN, CDKN2A*, and *CDH1*) due to genetic or epigenetic alterations have been characterized.

Gene expression studies have converged on major molecular classes of hepatocellular carcinoma by analyzing patients at different stages and with different etiologic factors (3–8). One class is associated with high proliferation, chromosomal instability, and activation of insulin-like growth factor (IGF) or Akt/mammalian target of rapamycin signaling. Another class features activation of the Wnt signaling pathway associated with a high prevalence of mutations in *CTNNB1*, which is the gene with the second highest frequency of known mutations in hepatocellular carcinomas, after *TP53* (7, 9). Mutations or deletions in *CTNNB1* exon 3 prevent the ubiquitination of its protein product, β-catenin, leading to its nuclear translocation and *trans*-activation of target genes (10). A third class is associated with IFN signaling due to leukocyte infiltration (4). Intriguingly, an interleukin gene expression signature from the adjacent liver tissue has also been linked to higher rates of venous invasion and metastasis, pointing to the importance of tumor microenvironment in the genesis and intrahepatic dissemination of hepatocellular carcinoma (11). Despite all these efforts, only two studies have been able to correlate homogeneous biological tumor patterns with survival outcomes (5, 8), although confirmatory-independent validations are not yet available. In parallel, genome-wide chromosomal aberration studies (12–16) and methylation studies (17) have begun to decipher the molecular heterogeneity of hepatocellular carcinoma.

The increasing worldwide incidence of hepatocellular carcinomas due to chronic hepatitis C infection underscores the need to

discover biomarkers for early detection and tumor progression, as well as gene targets for primary and adjuvant therapies. We conducted extensive genomic and transcriptomic characterization of tumors from hepatitis C virus–positive patients with early disease, as defined by a clinical staging system. We show that high-level copy number gain of 6p21 represents one mechanism for increasing vascular endothelial growth factor A (VEGFA) expression. In addition, we define five molecular classes that integrate copy number and gene expression alterations with signaling pathway assessment and describe a new molecular class defined by increased dosage of chromosome 7 and overexpression of oncogenes on this region.

Materials and Methods

Primary hepatocellular carcinoma specimens. Fresh frozen tissue specimens measuring 1 cm^3 were obtained at the time of surgical resection or liver transplantation from 100 anonymous patients from the HCC Genomic Consortium (Barcelona Hospital Clinic, Milan National Cancer Institute, and Mount Sinai School of Medicine) according to institutional review board–approved protocols. Two nodules were obtained from each of three transplantation patients, for a total of 103 tumor samples. For 94 of these samples, uninvolved cirrhotic tissue was obtained from the same patient at time of surgery. Clinicopathologic annotated data were analyzed in 82 samples obtained from surgical resection (Supplementary Table S1). Hepatitis C virus infection was confirmed by serology in all cases, and other etiologies of hepatocellular carcinoma were ruled out. Tissue samples were treated with RNAlater (Qiagen) or liquid nitrogen and stored at −80°C until DNA and RNA extraction, as previously reported (18). Genomic DNA was extracted with the ChargeSwitch gDNA mini kit (Invitrogen) and further purified with phenol-chloroform extraction. An independent set of 210 hepatocellular carcinoma patients from all etiologies undergoing resection was included to validate high-level gains of *VEGFA* by fluorescence *in situ* hybridization (FISH) of tissue microarrays (Supplementary Table S1).

Single-nucleotide polymorphism arrays. Genotypes and hybridization intensities for more than 238,000 single-nucleotide polymorphisms (SNP) were measured with the StyI chip of the Affymetrix 500K Human Mapping Array set (Affymetrix). Data were analyzed with the GenePattern software package (19) according to methods previously described (20). Intensity (.CEL) files were normalized with invariant-set normalization and modeled using the PM-MM difference modeling method with the SNPFileCreator module (19). Copy numbers were inferred by comparing signal intensities between each tumor and a selection of the five most similar normals selected from nontumoral cirrhotic tissue, as well as a database of multiple tumor types (21). The similarity between tumor and normal profiles was measured as the Euclidean distance between the log 2–transformed signal profiles (21).

Statistical analysis of copy number alterations. Copy number data were preprocessed with GISTIC software, which includes steps for batch correction, data normalization, copy number estimation versus the average of the five closest normal samples, and copy number segmentation (refer to supplement of ref. 21). Copy number alterations at each probe set i are evaluated by the score $G_i = f_i\, a_i$, where a_i represents the average amplitude of gain or loss with an overall frequency f_i in the data set. We used copy number cutoffs of 2.2 to detect broad regions of copy gain and 1.8 for loss because these cutoffs exceeded the variation observed in adjacent cirrhotic tissues obtained from the same patients. We obtained similar results by inferring copy numbers with the GEMCA algorithm (Supplementary Fig. S5; ref. 22). To detect high-level gains, we raised the copy number threshold to 3.8 copies (20).

FISH. Four-micron-thick tissue sections were mounted on standard glass slides and baked at 60°C for 2 h. Slides were deparaffinized, dehydrated, and the tissue sections treated with Digest-All III solution (Invitrogen) according to standard protocols. Commercial α-satellite probes corresponding to the centromeric regions of chromosome 6 (CEP-6) or chromosome 11 (CEP-11) were purchased prelabeled with SpectrumGreen dUTP (Abbott Molecular/Vysis, Inc.). One microgram each of BACs corresponding to the *VEGFA* (RP11-710L16) or *CCND1* (RP11-156B3) loci was directly labeled with SpectrumOrange dUTP using nick translation (Abbott Molecular/Vysis), then hybridized and washed using standard protocols. Slides were imaged using Olympus BX51 fluorescence microscope and the Applied Imaging system running CytoVision Genus version 3.9 (Supplementary Methods).

Tissue microarrays. Tissue microarrays were constructed using the Advanced Tissue Arrayer ATA-100 (Millipore). Targets for arraying were identified by a liver pathologist (S.T.) by marking the morphologically more representative areas chosen from H&E-stained sections from each paraffin block. Two tissue cores with a diameter of 1.5 mm were transferred from each donor block to the recipient tissue microarray.

Quantitative real-time PCR. Total RNA was extracted from three to four tissue sections, each 10 μm thick, using the TRIzol LS reagent (Invitrogen). cDNA synthesis and PCR conditions were conducted as previously described (23). Expression levels were measured with TaqMan probes Hs00173626-m1 for VEGFA and Hs03023943-g1 for ACTB obtained from TaqMan Gene Expression Assays (Applied Biosystems). Reactions were set up as triplicates for each gene, and the median threshold cycle (C_t) value from the triplicates was used. We calculated ΔC_t values between VEGFA and ACTB for each tumor, and $\Delta\Delta C_t$ values were calculated between the ΔC_t for each tumor and the median ΔC_t for five uninvolved, noncancerous cirrhotic controls. The Mann-Whitney test was used to evaluate differences in expression levels between groups.

Affymetrix U133 Plus 2.0 expression data. Gene expression assessment was done in 91 tumor samples: 69 new samples obtained from surgical resection extracted as described previously and additional 22 tumor samples and 8 cirrhotic liver controls already reported (18). Affymetrix array intensity (.CEL) files were processed with the RMA algorithm (24). To compare expression levels across microarray platforms, we remapped probe sequences on each platform to AceView transcripts (25, 26). Array intensity data (.CEL files) have been deposited in the National Center for Biotechnology Information Gene Expression Omnibus[12] and are accessible through Gene Expression Omnibus Series accession no. GSE9829.

Unsupervised classification of gene expression data. We adopted a robust hierarchical clustering approach for unsupervised classification of Affymetrix U133Plus 2.0 data (7). We averaged the results from modifying three clustering parameters: transcript lists, linkage method, and number of clusters (see Supplementary Methods). The reproducibility of hierarchical clustering was assessed with the GenePattern ConsensusClustering module, version 3, using a 1 − Pearson correlation distance metric after mean-centering of genes (27).

Selection of class-specific marker genes. For each of the five gene expression classes obtained from consensus hierarchical clustering, we performed supervised analysis to identify genes that were significantly up-regulated or down-regulated among tumors. Significance Analysis of Microarrays with 500 permutations of class labels evaluated the significance of gene expression changes that were significantly overexpressed or underexpressed among the tumors in a single class. Up to 200 overexpressed transcripts and up to 200 underexpressed transcripts with a ≥2-fold change and a false discovery rate (FDR) $q < 0.01$ were selected as marker genes. The list of marker genes for each class is provided in Supplementary Tables S6 to S10.

Cross-dataset prediction of gene expression classes. Affymetrix U133A array data were obtained from EBI ArrayExpress, with accession no. E-TABM-36 (7). These U133A array probe sets were mapped to 12,145 AceView transcripts based on exact sequence matches (25). NCI-Operon oligonucleotide microarray data were obtained from Gene Expression Omnibus, with accession nos. GSE1898 and GSE4024 (5, 6). The Prediction Analysis of Microarrays R package was used to train shrunken centroid classifiers from previously published gene expression data and class labels (see Supplementary Methods; ref. 28).

[12] http://www.ncbi.nlm.nih.gov/geo

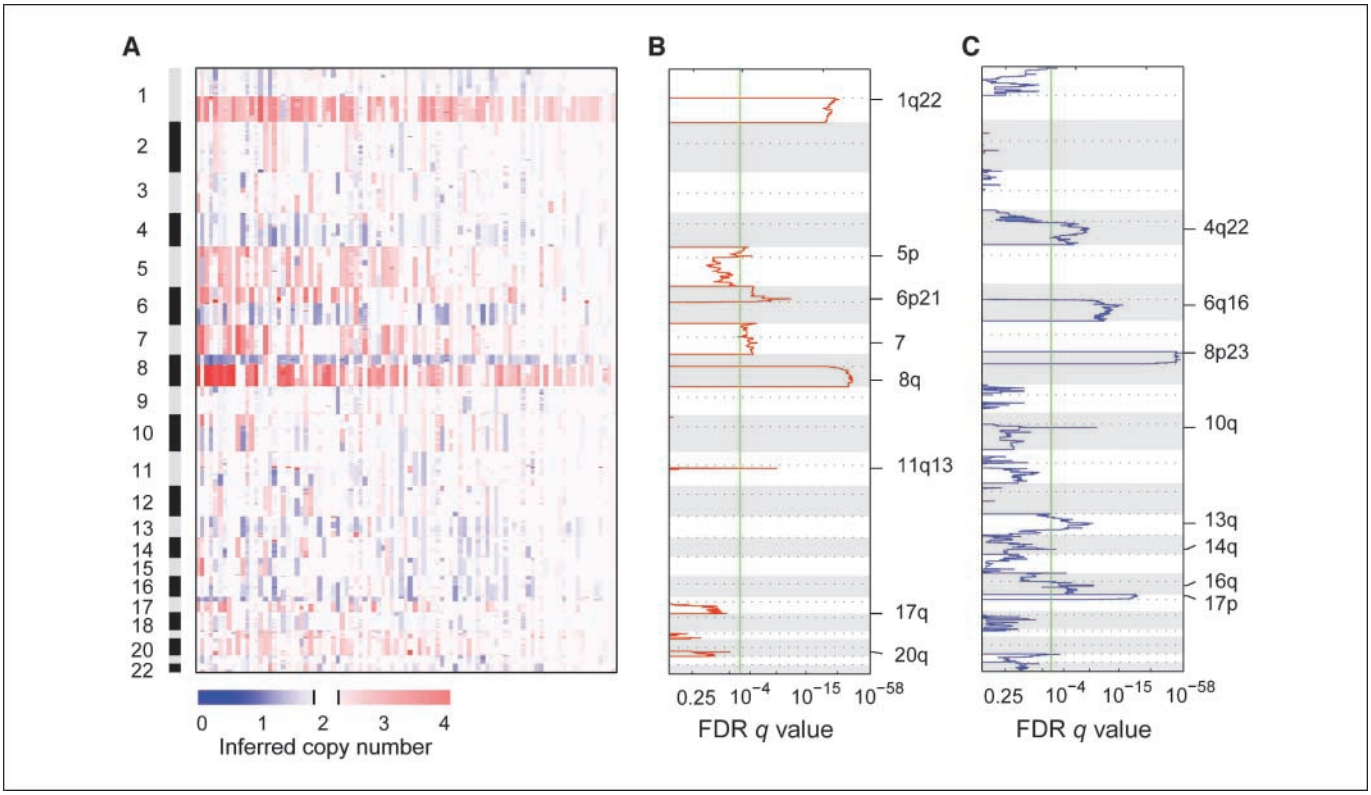

Figure 1. Copy number alterations in hepatocellular carcinomas arising from hepatitis C viral infection. *A,* overview of chromosomal gains and losses in 103 hepatocellular carcinomas. Each tumor is displayed in a separate column, and inferred copy numbers at 238,304 loci are displayed from top to bottom in genomic order. Tumors are ordered from left to right according to the number of chromosome arms with significant copy number alterations. *Red,* copy number gains; *blue,* copy number losses. *B,* recurrent chromosomal gains. *C,* recurrent chromosomal losses. The GISTIC algorithm identified significant regions of copy number alterations in multiple samples. Chromosomes are displayed in ascending order along the vertical axis. *Horizontal axis,* statistical significance of recurrent gains or losses, corresponding to the FDR *q* value obtained from GISTIC. *Vertical green line,* significance threshold of $q < 0.001$.

Sequencing. PCR and sequencing were conducted by GENEWIZ. PCR primers and reaction conditions are listed in Supplementary Table S12 and Supplementary data. Mutations were detected by Mutation Surveyor 2.51 (SoftGenetics), followed by manual review of candidate mutations.

Immunohistochemistry. Formalin-fixed, paraffin-embedded sections were used to assess phosphorylated proteins in human tissue. Sections placed on glass were baked at 60°C for 30 min, deparaffinized in xylene, and rehydrated in a graded series of ethanol solutions. Antigens were unmasked by microwave heating the samples in 10 mmol/L sodium citrate buffer (pH 6.0) for 5 min (×3). Endogenous peroxidase from the tissue was quenched with 3% hydrogen peroxide. After washing with PBS, samples were incubated with anti–phosphorylated (Ser^{473}) Akt antibody (1:50; immunohistochemistry specific, Cell Signaling Technology), anti–phosphorylated (Tyr^{1316}) IGF-I receptor (IGF-IR; 1:100; Dr. Rubini, University of Ferrara, Ferrara, Italy), anti-CTNNB1 (1:750; Abcam), or anti–phosphorylated ($Ser^{240/244}$) RPS6 (1:200; Cell Signaling Technology) at 4°C overnight. 3,3′-Diaminobenzidine was used as a detection system (EnVision+ System-HRP, DAKO). Immunoreactivity was independently graded by two liver pathologists (S.T. and M.S.) and both agreed in the final staining score. The variables measured were as follows: (*a*) intensity (0, absent; 1, weak; 2, moderate; 3, strong); (*b*) distribution (1, very focal; 2, focal; 3, diffuse); and (*c*) localization of the staining (membranous, cytoplasmic, or nuclear). Samples were defined positive for Akt or IGF-IR phosphorylation when intensity was ≥2, regardless of distribution. For RPS6 phosphorylation, only those samples with intensity and distribution of ≥2 were considered positive. Tumors with CTNNB1 activation were defined by the presence of nuclear staining or by >5% of cytoplasmic staining.

Statistical associations. Each of the five gene expression classes was assessed for enrichment with molecular characteristics. Fisher's exact test was used to assess the enrichment of binary variables such as immunostaining, mutation status, and chromosomal gain or loss. The Mann-Whitney was used to test for associations with continuous variables, such as α-fetoprotein (AFP) levels.

Analysis of clinical outcomes. The probability curves of recurrence and early recurrence were calculated according to Kaplan-Meier and compared by Mantel-Cox test. Median inferred copy numbers for chromosomal arms for each sample were used as covariates for univariate association with recurrence. Median copy numbers of chromosomal arms were calculated for each tumor sample, and cutoffs of 2.2 for copy gains and 1.8 for copy loss were used. For continuous variables, the cutoff level was their median value. Significant variables ($P < 0.05$) were included in a stepwise Cox proportional hazard regression analysis of recurrence and early recurrence. The calculations were done with the SPSS package (SPSS 15.0).

Results

Copy number alterations in clinically early, HCV-related hepatocellular carcinomas. We measured copy number alterations at over 238,000 genomic loci with Affymetrix Sty mapping arrays among 103 primary tumors. According to the Barcelona Clinic Liver Cancer staging system, 80% of these patients had very early or early stage disease (stage 0 or stage A), representing asymptomatic tumors with either a single nodule or up to three nodules <3 cm in diameter (Supplementary Table S1; ref. 29). To find evidence for driver alterations in tumor genomes, we evaluated the frequency and magnitude of copy number gains and losses with the GISTIC algorithm (21). Broad gains and losses of chromosome arms were the most prevalent changes among these tumors (Fig. 1*A*). The most significant chromosomal gains affected

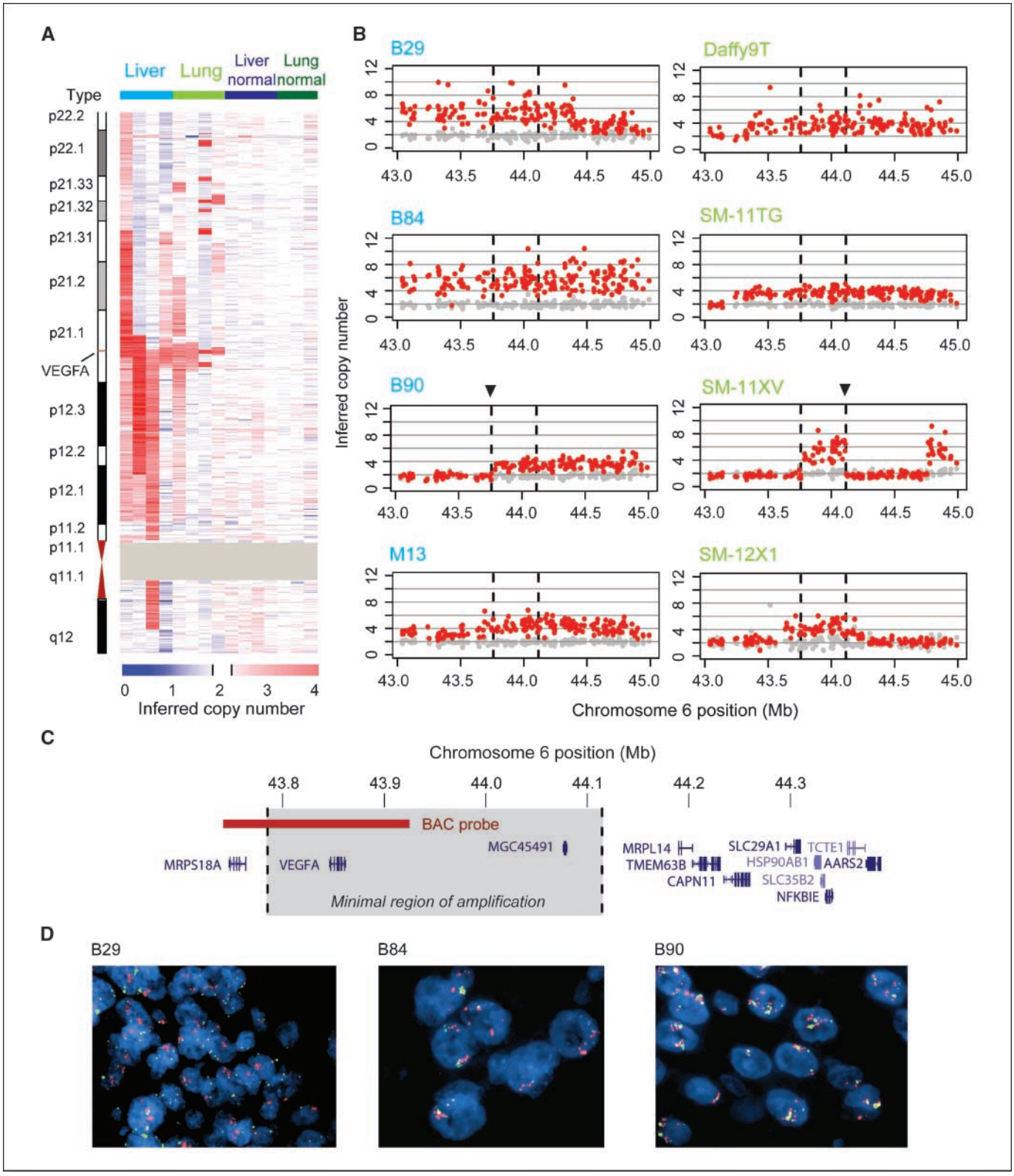

Figure 2. Overlapping high-level gains at 6p21 in hepatocellular carcinomas and lung adenocarcinomas. *A,* copy number alterations among four hepatocellular carcinomas (*light blue*), four lung adenocarcinomas (*light green*), four matched cirrhotic tissues from adjacent liver (*dark blue*), and three matched normals for the lung tumors (*dark green*). *B,* inferred copy numbers at individual SNP probe sets. Copy numbers are shown in red for tumor samples or in gray for the matched normal from the same patient. Vertical dashed lines delineate the boundaries of the minimal overlapping region among the eight tumors. *C,* annotated genes found in the minimal overlapping region at 6p21. Inclusion of the SM-11XV lung tumor narrows the overlapping region to the boundaries of the shaded box. The genomic location of BAC probe RP11-710L16 used for FISH is indicated. *D,* confirmation of *VEGFA* copy gains by FISH. *Red signals,* BAC probe RP-710L16 centered on *VEGFA*; *green signals,* BAC probe CEP-6 for the centromere of chromosome 6. Representative images are displayed for the three of four hepatocellular carcinomas with available tissue blocks, and detailed counts of probe signals are provided in Supplementary Table S4.

Table 1. FISH analyses of 6p21 copy number alterations in 210 hepatocellular carcinomas on tissue microarrays

Copy number alteration	*n* (%)	Mean VEGFA probe signals	Mean CEP6 probe signals	VEGFA/CEP6 ratios
VEGFA amplifications	2 (1.0)	6.5–14.9	2.1–2.1	4.1–7.2
VEGFA high-level gains	14 (6.7)	4.0–6.5	2.1–5.9	1.1–1.8
Chromosome 6 gains	58 (27.6)	2.3–3.9	2.0–3.7	1.0–1.8
Normal chromosome 6	136 (64.8)			

chromosome arms 1q (72%) and 8q (66%), which are early events in hepatocarcinogenesis (Fig. 1*B*; ref. 30). Focal gains centered on 6p21 (4%) and 11q13 (6%) were the next most significant alterations due to their high levels of copy increase. Significant copy number gains were also observed for chromosomes 5p (33%), 7 (30%), 17q (19%), and 20 (18%). Notably, gains of chromosomes 5p and 7 significantly co-occurred among these tumors ($P < 10^{-4}$, Fisher's exact), which may indicate cooperation among multiple genes with elevated dosage on both chromosomes. Significant chromosomal losses affected chromosome arms 8p (60%), 17p (39%), 6q (27%), 4q (19%), 13q (19%), 16q (17%), 14q (13%), and 10q (11%; Fig. 1*C*). Aside from 1q gain, 8q gain, and 8p loss in the majority of tumors, substantially lower frequencies of gains and losses on other chromosome arms suggested the presence of multiple tumor subtypes that select for alterations in distinct signaling pathways. We did not detect chromosomal gains or losses in the 94 uninvolved, noncancerous cirrhotic tissue samples (Supplementary Fig. S4*D*).

Focal regions of copy gain or loss provide greater resolution to map oncogenes or tumor suppressors by narrowing the overlapping genomic region among multiple tumors. However, these focal lesions were rare events among clinically early hepatocellular carcinomas. Only 15% of tumors harbored at least one high-level gain, which we define as a genomic region smaller than 12 Mb with inferred copy number >3.8 (Supplementary Table S2). We found 9 candidate regions of homozygous deletion, all of which

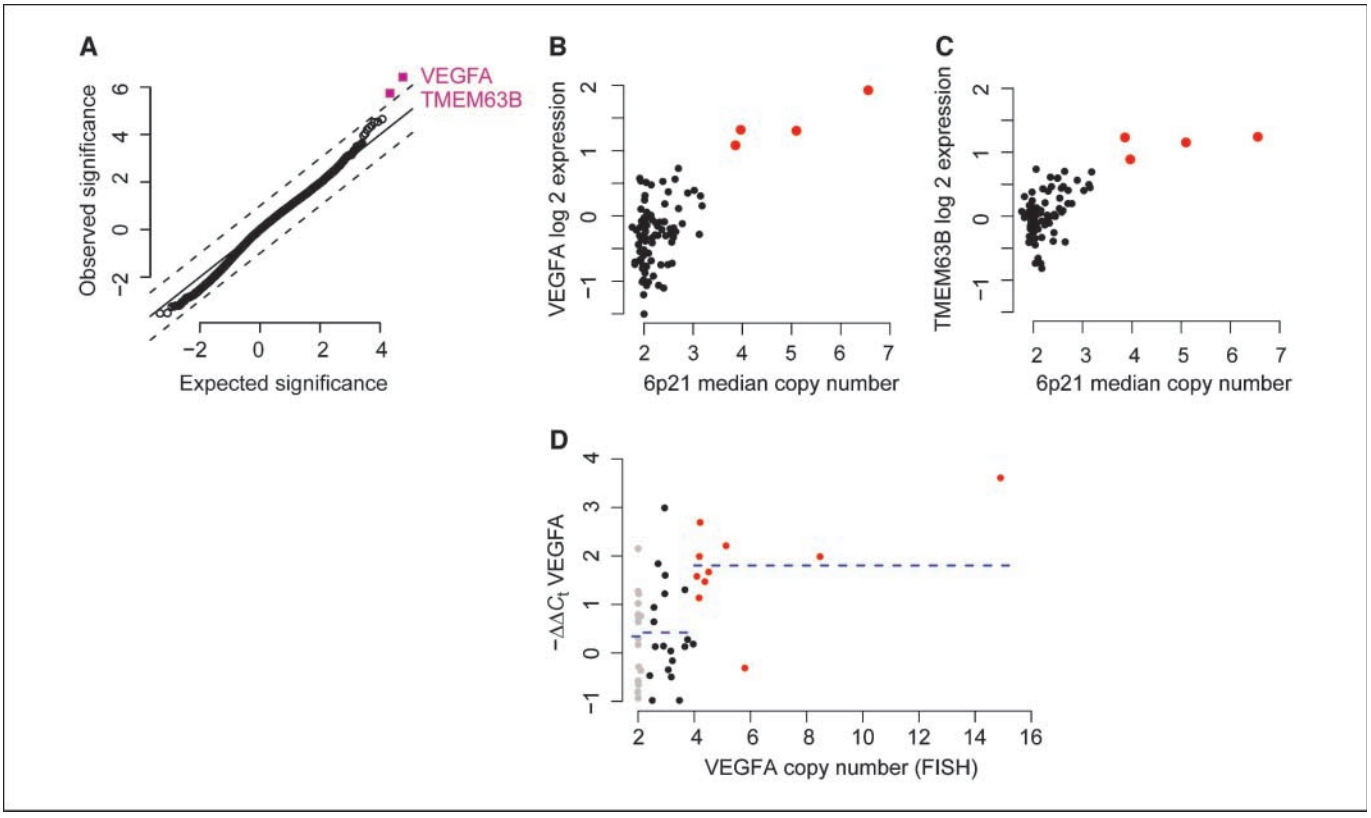

Figure 3. High-level gains at 6p21 lead to VEGFA overexpression. *A,* Significance Analysis of Microarrays identified overexpression of two genes among the four tumors with 6p21 amplifications. Each point represents the observed *t* statistic, plotted against its expected score from permutation tests. The most significant gene is *VEGFA*, followed by *TMEM63B* (*purple*). *Dashed lines,* confidence interval for the random, null distribution. VEGFA (*B*) or TMEM63B (*C*) is overexpressed in tumors with high-level gains of 6p21. Each of the 91 points represents the corresponding copy number and expression level for a single tumor. *Horizontal axis,* median inferred copy number for 68 SNP probes in the minimal overlapping region at 6p21. *Vertical axis,* log 2 ratio between the expression level of each tumor, compared with the median of 10 normal liver samples on the Affymetrix U133 Plus 2 array. *D,* higher VEGFA expression is associated with increased copy numbers in an independent cohort. Each of the 45 points represents a single tumor chosen from the panel of 210 tumors evaluated by FISH. *Horizontal axis,* average number of *VEGFA* probes per nucleus. *Vertical axis,* negative $\Delta\Delta C_t$ values of VEGFA normalized to ACTB, compared with the median of five uninvolved, cirrhotic tissue samples. *Red,* tumors with >4 copies of *VEGFA* ($n = 10$); *black,* tumors with gains of chromosome 6 ($n = 19$); *gray,* diploid tumors ($n = 16$). The average negative $\Delta\Delta C_t$ value for each of these three classes is plotted with a dashed blue line.

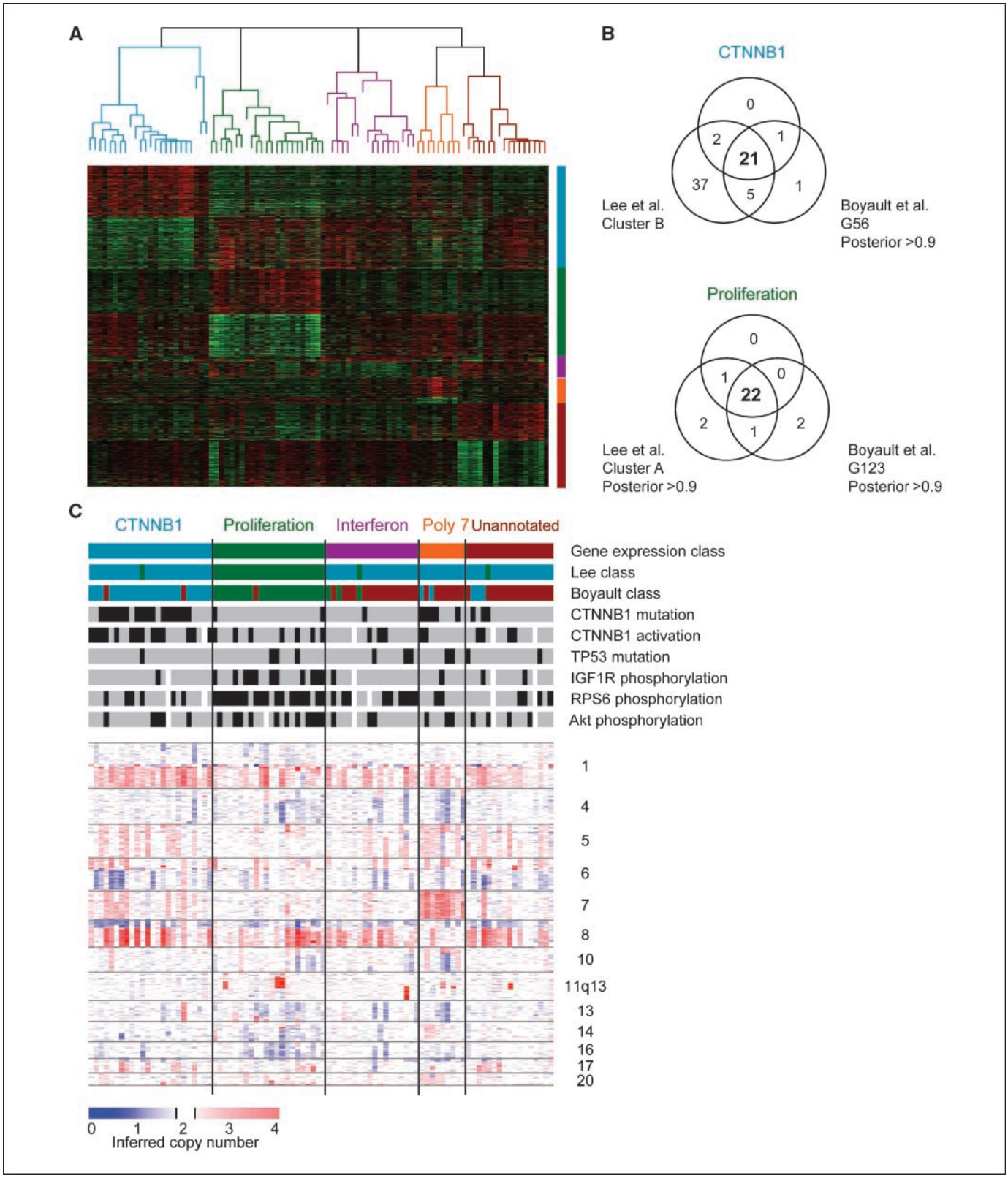

Figure 4. Integrated classification of genomic and molecular alterations in hepatocellular carcinomas. *A,* consensus hierarchical clustering of gene expression in 91 tumors. Colors in the sample dendrogram indicate the five gene expression classes determined by consensus hierarchical clustering among 32 different parameter set combinations. Rows display mean-centered expression levels for 1,242 marker genes associated with each of the five gene expression classes. *B,* overlap of consensus classes with previously published classes. Class labels were assigned based on the distance to the closest shrunken centroid classifier for previous classifications (5, 7). *C,* copy number alterations among the gene expression classes. Gains and losses for the indicated chromosomes are displayed according to the color scheme in Fig. 2. Mutation status (*CTNNB1* exon 3 or *TP53* exons 5–8) and immunohistochemical staining are indicated in grayscale: present (*black*), absent (*gray*), or missing (*white*) data.

Table 2. Variables with independent predictive value for clinical outcomes in multivariate analysis

	Early recurrence		Overall recurrence	
	Hazard ratio (95% CI)	*P*	Hazard ratio (95% CI)	*P*
Barcelona-Clinic Liver Cancer staging classification	8.8 (4.3–17.6)	<0.001	7.1 (3.8–13.5)	<0.001
Chromosome 7 median copy number >2.2	5.8 (2.4–13.8)	<0.001	3.4 (1.7–6.8)	<0.001

Abbreviation: 95% CI, 95% confidence interval.

occurred in only one tumor (Supplementary Table S3). Two of these regions affected single exons of *CSMD1* or *MSR1*, whereas two regions deleted exons of *GPR143, SHROOM2, WWC3, MAOA*, and *MAOB*.

To pinpoint genomic regions that may harbor key oncogenes, we repeated GISTIC analysis to find significantly recurrent high-level gains. The most frequent amplifications occurred in six tumors at 11q13, with a minimal common region from 68.83 to 69.30 Mb (FDR $q < 10^{-11}$; Supplementary Fig. S1). This region included only four known genes: *CCND1, ORAOV1, FGF19*, and *FGF4*. FISH with a BAC probe to these four genes confirmed that all three of these tumors with available tissue blocks harbored amplifications. In 50% to 90% of tumor nuclei, more than 10 signals corresponding to BAC RP11-710L16 were detected (Supplementary Fig. S1).

Overlapping high-level gains at 6p21 occur in multiple tumor types. The second most frequent high-level gains pinpointed an overlapping region that had not previously been described in hepatocellular carcinomas (FDR $q < 10^{-11}$). Four tumors harbored high-level gains of 6p21, ranging in size from 2.4 to 22 Mb (Fig. 2*A* and *B*). Remarkably, a recent study of 371 lung adenocarcinomas identified this locus as the 17th most frequent region of copy gains, yet this frequency barely passed statistical significance (FDR $q < 0.08$; ref. 20). Assuming that the same oncogene targets are under selection in multiple tumor types (31), we pooled regions of high-level gains from four hepatocellular carcinomas and four lung adenocarcinomas. The minimal region of overlap, between positions 43.792 and 44.110 Mb, encompassed only two genes, *VEGFA* and *MGC45491* (Fig. 2*C*).

High-level gains of 6p21 were confirmed in two FISH studies with a BAC probe spanning the *MRPS18A* and *VEGFA* genes (Fig. 2*C*). First, FISH analysis on thin sections from all three hepatocellular carcinomas with available tissue blocks validated copy gains at 6p21, with an average of >5.5 *VEGFA* probe signals per tumor (Fig. 2*D*; Supplementary Fig. S2; Supplementary Table S4). Second, we also performed FISH analysis on an independent tissue microarray collection of 210 hepatocellular carcinomas (Table 1; Supplementary Table S1; Supplementary Table S4). We defined three cytogenetic categories based on the average number of *VEGFA* probe signals observed per nucleus. Gains of chromosome 6 were found in 58 of 210 (27.6%) tumors, with ≥2.3 probe signals. An additional 14 (6.7%) tumors also had high-level gains of *VEGFA*, as defined by ≥4 *VEGFA* probe signals. Two tumors showed *VEGFA* amplifications (1.0%), with >8 *VEGFA* probe signals.

***VEGFA* is a likely oncogene target of high-level gains at 6p21.** Genomic regions with increased copy number are often retained in tumor cells due to selective advantages conferred by the increased expression of one or more target genes residing in the region. To identify candidate oncogene targets in the overlapping regions of copy gains at 6p21 and 11q13, we evaluated the association between copy numbers at these loci and the expression of each gene. A genome-wide, permutation-based *t* test identified only two known genes that were significantly overexpressed among the four tumors with high-level gains at 6p21: *VEGFA* and *TMEM63B* (FDR $q < 0.001$; Fig. 3*A*). *VEGFA* was the most significantly overexpressed transcript, with an average 2.8-fold higher expression among the four tumors with 6p21 high-level gains (Fig. 3*B*). *TMEM63B* encodes a transmembrane protein with unknown function, and the four tumors with 6p21 high-level gains had 1.9-fold higher average expression (Fig. 3*C*). Thus, elevated levels of TMEM63B may represent a marker indicating VEGFA overexpression by increased copy dosage, rather than VEGFA overexpression due to *trans*-regulation by hypoxia-inducible factor 1A or other regulators.

Notably, VEGFA expression was also associated with copy numbers measured by FISH among 45 tumors in the tissue microarray cohort. Ten tumors with >4 copies of *VEGFA* had an average of 2.8-fold higher expression than 16 tumors that were diploid at this locus ($P = 0.0007$, Mann-Whitney; Fig. 3*D*). Thus, we have validated that high-level gains of *VEGFA* are associated with higher VEGFA expression in two independent cohorts.

For the six tumors with 11q13 amplifications, we found four genes to be significantly overexpressed: *ORAOV1, TPCN2, CCND1*, and *MRPL21* (FDR $q < 0.001$). Both *ORAOV1* and *CCND1* reside in the minimal common region of amplification. *CCND1* is a confirmed oncogene in hepatocarcinogenesis (32), whereas the log expression levels of *ORAOV1* showed a strikingly linear correlation with the median copy number of 11q13 (Supplementary Fig. S1*D*).

Gene expression classes are associated with signaling pathway alterations. To characterize the molecular heterogeneity of hepatocellular carcinomas, we measured gene expression profiles in 91 of the 103 tumors with oligonucleotide microarrays (Affymetrix U133 Plus 2 arrays). We obtained five gene expression classes from unsupervised classification with consensus hierarchical clustering, which considered 32 different parameter combinations (Fig. 4*A*; ref. 7). To validate these five gene expression classes with previously published studies, we trained shrunken centroid classifiers on two additional gene expression data sets (6, 7). Two classes showed extremely good concordance with the labels predicted by these external classifiers (Fig. 4*B*). Furthermore, signaling pathway annotations could be assigned for three of these five classes by the enrichment of marker genes, immunohistochemistry, and mutations (Fig. 4*C*; Supplementary Tables S5–S10).

The high prevalence of *CTNNB1* mutations indicated alterations to canonical Wnt signaling in a subset of hepatocellular carcinomas. The *CTNNB1*-associated class of 24 tumors was signifi-

cantly enriched for *CTNNB1* exon 3 mutations (62%; $P < 6 \times 10^{-4}$, Fisher's exact) and nuclear localization (71%; $P < 3 \times 10^{-5}$, Fisher's exact; Supplementary Table S5). Further evidence for CTNNB1 activation among tumors in this class came from the significant overexpression of several liver-specific marker genes including *GLUL, LGR5, TBX3*, and *REG3A* (Supplementary Table S6; refs. 33–35). This class was also associated with tumor diameters >3 cm ($P = 0.002$, Fisher's exact).

Another molecular subtype of hepatocellular carcinomas featured increased proliferation, high levels of serum AFP, and chromosomal instability (5, 7). We found a corresponding proliferation class of 23 tumors that overexpressed AFP (median serum level, 472 ng/mL; $P = 0.001$, Mann-Whitney), along with several genes corresponding to a proliferation gene expression signature (Supplementary Tables S5 and S7; ref. 36). Because these tumors were enriched for IGF-IR phosphorylation (48%; $P < 1 \times 10^{-4}$, Fisher's exact), RPS6 phosphorylation (83%; $P = 0.003$, Fisher's exact), and Akt phosphorylation (55%; $P = 0.01$, Fisher's exact), it is likely that tyrosine kinase activation drives the proliferation of these tumors. Reduced frequencies of *CTNNB1* exon 3 mutations among these tumors (13%; $P = 0.02$, Fisher's exact) confirmed the model that tyrosine kinase activation and *CTNNB1* activation represent distinct routes for tumor progression (7, 37). Tumors in this class also had higher frequencies of 4q loss (38%; $P = 0.03$, Fisher's exact) and 13q loss (33%; $P = 0.04$, Fisher's exact), as well as lower frequencies of 6q loss (12%; $P = 0.04$, Fisher's exact). A significant correlation with macrovascular invasion was observed for tumors in this proliferation class ($P = 0.007$, Fisher's exact).

A third class of 18 tumors also harbored significantly lower rates of *CTNNB1* exon 3 mutation (6%; $P = 0.004$, Fisher's exact). Lower expression of IGF-II, as well as CTNNB1 target genes, suggested that these tumors represent a distinct class. Strikingly, 4 of the 28 significantly overexpressed marker genes corresponded to IFN-stimulated genes: *STAT1, ISG15, IFI6*, and *IFI27* (Supplementary Table S8; ref. 38). STAT1 is a transcription factor that mediates the response to hepatitis C viral infection, whereas elevated expressions of ISG15, IFI6, and IFI27 are predictive markers of hepatitis C virus patients who failed to respond to pegylated IFN and ribavirin therapy (39). Notably, tumors about this IFN-related class were more likely to be <3 cm in diameter ($P = 0.005$, Fisher's exact).

Polysomy of chromosome 7 defines a novel gene expression class. We discovered a new class of 9 tumors that was significantly associated with a lack of gains of chromosome 8q (78%; $P = 0.007$, Fisher's exact), as well as polysomy of chromosome 7 above a median copy number of 2.7 (89%; $P < 10^{-8}$, Fisher's exact). Increased dosage led to significantly higher expression levels of multiple genes on chromosome 7 (Supplementary Table S9), as confirmed by gene set enrichment analysis based on cytobands (FDR $q < 0.01$). The most significantly overexpressed genes on chromosome 7 included *COBL, CLDN15, MAD1L1, POLD2*, and *EPHA1*, although oncogene targets of these high-level gains remain to be identified. Due to the small number of tumors in this class, we lacked the power to detect significant clinicopathologic correlations.

Prognostic significance of genomic alterations. We evaluated associations between copy number alterations and clinical outcomes among 82 patients who underwent surgical resection. Recurrence was associated with chromosome 7 gain and 13q loss by univariate analysis (Supplementary Table S11). On multivariate analysis, chromosome 7 gain was retained as an independent predictor of recurrence [hazard ratio, 3.4 (95% confidence interval, 1.7–6.8); $P < 0.001$], along with BCLC staging [hazard ratio, 7.1 (95% confidence interval, 3.8–13.5); $P < 0.001$]. Notably, gains of chromosome 7 were associated with a significantly higher risk of recurrence within 2 years (early recurrence) after surgical resection (Table 2; Supplementary Fig. S3).

Discussion

To date, this study represents the largest characterization effort of paired copy number and gene expression alterations in clinically early hepatocellular carcinomas with hepatitis C virus etiology. Combined annotations from marker gene lists, mutation analyses, and immunohistochemistry could associate three of five gene expression classes with previously described signaling pathway alterations (4, 5, 7). First, a CTNNB1-activated class was enriched for *CTNNB1* exon 3 mutations and immunohistochemical staining. Second, a proliferation class was enriched for IGF-IR and RPS6 phosphorylation, thus pointing to potential targets for combined therapeutic strategies. Small-molecule inhibitors and monoclonal antibodies against IGF-IR [such as A12 (Imclone)] and mammalian target of rapamycin [such as rapamycin or everolimus (Novartis)] are still at preclinical or early clinical stage of drug development for hepatocellular carcinoma (40). Third, an IFN-related class that overexpressed several IFN-stimulated genes was associated with smaller tumor size. Notably, tumors with up-regulated IFN response in another study also had higher leukocyte infiltration and tumor apoptosis (4).

A novel gene expression class was defined by polysomy of chromosome 7 and the concomitant overexpression of multiple genes along this chromosome. Intriguingly, most of these tumors lacked 8q gains, which are the second most frequent chromosomal alterations in hepatocellular carcinomas and include the known oncogenes *MYC, PTK2*, and *COPS5* (12, 41). This observation suggests that unknown target oncogenes on chromosome 7 may contribute to a distinct mechanism of tumor progression. Indeed, we found that even low-level gains of chromosome 7 were independent predictors of recurrence within 2 years of surgical resection. Although *EGFR* and *MET* are frequently cited oncogene candidates on chromosome 7, we only observed a modest overexpression of EGFR (1.39-fold versus normals) and MET (1.82-fold versus normals) among the nine tumors in this class. Surprisingly, we did not observe amplifications of *MET* among these hepatitis C virus–positive tumors, although previous studies have reported a few instances of focal *MET* amplification, mostly in tumors arising in the context of hepatitis B virus infection (12, 13, 31). Thus, this discrepancy in *MET* amplification or overexpression could be explained by differences in viral etiologies or accompanying cirrhosis.

Due to the limited number of patients and events in each class, the size of this cohort was underpowered to detect robust differences in overall survival, and only correlation with metastatic potential was captured. Nevertheless, we speculate that these gene expression classes may represent distinct combinations of signaling pathway alterations and would thus show different responses to molecular targeted therapies. Thus, biomarkers for hepatocellular carcinoma molecular classes should be assayed in future clinical trials to provide evidence of treatment response in a genetically defined subset of patients. In addition, animal models that recapitulate these molecular classes should be instrumental for testing novel antitumoral agents in preclinical experiments. For instance, a double transgenic *MYC/TGFA* mouse model of hepatocellular carcinoma has similar gene expression patterns

with human tumors in the proliferation class (42). Additional mouse models that recapitulate the remaining classes need to be characterized.

We propose that high-level gains of *VEGFA* may represent a genetic dependency of tumors arising in multiple tissue types, and that these high-level gains may predict response to a variety of inhibitors against VEGFA or its receptors. Whereas chromosome 6p gains have previously been reported in hepatocellular carcinoma (30, 43), the higher resolution of SNP arrays in this study has localized a minimal common region of copy gains that included *VEGFA*. We also found that three of the four tumors with focal gains of 6p21 were assigned to an unannotated gene expression class.

Although the prognostic significance of elevated transcript and serum VEGFA levels in early hepatocellular carcinomas has been recognized (44, 45), this study is the first report of focal copy gains as a mechanism for elevated VEGFA expression. Intriguingly, KDR/VEGFR-2 and FLT4/VEGFR-3 are among the putative targets of sorafenib (IC_{50} of 20–90 nmol/L), a multikinase inhibitor that has recently been shown to extend survival of patients with advanced hepatocellular carcinoma (46, 47). In contrast to the cell-autonomous effects of most oncogenes, high-level gains of *VEGFA* suggest that tumors may also select for genetic alterations that mediate tumor-stromal interactions. VEGFA can mediate at least two signals among epithelial and endothelial cells. Proliferating hepatocytes stimulate angiogenesis in a partial hepatectomy model by secreting VEGFA, which binds to FLT1 or KDR on sinusoidal endothelial cells (48). Conversely, VEGFA-activated endothelial cells can also produce hepatocyte growth factor in response to increased VEGFA levels, and this elevation stimulates hepatocyte proliferation (49). As further evidence for the paracrine effects of VEGFA, RNA interference against VEGFA did not affect proliferation of the SMMC-7221 hepatocellular carcinoma cell line *in vitro* but inhibited tumor growth and induced apoptosis in nude mice xenografts (50).

In conclusion, our integrated molecular classification encapsulates key signaling pathway alterations of HCV-related hepatocellular carcinomas. With their high concordance with other gene expression studies, these classes should be assayed for stratified analyses of future clinical trials. In addition, focal copy number gains and overexpression of *VEGFA*, as well as multiple genes on chromosome 7, suggest potential targets for molecular therapies.

Disclosure of Potential Conflicts of Interest

J.M. Llovet: commercial research grant, Bayer Pharmaceuticals; consultant/advisory board: Bayer Pharmaceuticals, Bristol Myers Squibb, and Johnson and Johnson. M. Meyerson: consultant, Novartis. V. Najfeld: speakers bureau/honoraria, Pharmion/Celgene. The other authors disclosed no potential conflicts of interest.

Acknowledgments

Received 2/27/2008; revised 5/19/2008; accepted 6/20/2008.

Grant support: NIH grants DK076986 (J.M. Llovet), CA109038 (M. Meyerson), and DK037340 (S.L. Friedman); Samuel Waxman Cancer Research Foundation (J.M. Llovet); Spanish National Health Institute grant SAF-2007-61898 (J.M. Llovet); Institució Catalana de Recerca Avançada (J.M. Llovet); Instituto de Salud Carlos III grants PI 05/645 (J. Bruix) and FIS CM04/00044 (B. Minguez); Italian Association for Cancer Research (V. Mazzaferro); Davies Charitable Foundation (D.Y. Chiang); Fundación Pedro Barrié de la Maza (A. Villanueva); National Cancer Center (A. Villanueva); European Association for the Study of the Liver (A. Villanueva); Charles A. King Trust (Y. Hoshida); and Department d'Educació i Universitats de la Generalitat de Catalunya (J. Bruix). Ciberehd is funded by Instituto de Salud Carlos III.

The costs of publication of this article were defrayed in part by the payment of page charges. This article must therefore be hereby marked *advertisement* in accordance with 18 U.S.C. Section 1734 solely to indicate this fact.

We thank Rameen Beroukhim and Craig Mermel for assistance with the GISTIC algorithm, and Barbara Weir and Roel Verhaak for critical reading of the manuscript.

We dedicate this work to the memory of our friend and colleague, Eric Lemmer.

References

1. Thorgeirsson SS, Grisham JW. Molecular pathogenesis of human hepatocellular carcinoma. Nat Genet 2002;31:339–46.
2. Farazi PA, DePinho RA. Hepatocellular carcinoma pathogenesis: from genes to environment. Nat Rev Cancer 2006;6:674–87.
3. Chen X, Cheung ST, So S, et al. Gene expression patterns in human liver cancers. Mol Biol Cell 2002;13:1929–39.
4. Breuhahn K, Vreden S, Haddad R, et al. Molecular profiling of human hepatocellular carcinoma defines mutually exclusive interferon regulation and insulin-like growth factor II overexpression. Cancer Res 2004;64:6058–64.
5. Lee JS, Chu IS, Heo J, et al. Classification and prediction of survival in hepatocellular carcinoma by gene expression profiling. Hepatology 2004;40:667–76.
6. Lee JS, Heo J, Libbrecht L, et al. A novel prognostic subtype of human hepatocellular carcinoma derived from hepatic progenitor cells. Nat Med 2006;12:410–6.
7. Boyault S, Rickman DS, de Reynies A, et al. Transcriptome classification of HCC is related to gene alterations and to new therapeutic targets. Hepatology 2007;45:42–52.
8. Yamashita T, Forgues M, Wang W, et al. EpCAM and α-fetoprotein expression defines novel prognostic subtypes of hepatocellular carcinoma. Cancer Res 2008;68:1451–61.
9. Laurent-Puig P, Legoix P, Bluteau O, et al. Genetic alterations associated with hepatocellular carcinomas define distinct pathways of hepatocarcinogenesis. Gastroenterology 2001;120:1763–73.
10. Provost E, McCabe A, Stern J, Lizardi I, D'Aquila TG, Rimm DL. Functional correlates of mutation of the Asp32 and Gly34 residues of β-catenin. Oncogene 2005;24:2667–76.
11. Budhu A, Forgues M, Ye QH, et al. Prediction of venous metastases, recurrence, and prognosis in hepatocellular carcinoma based on a unique immune response signature of the liver microenvironment. Cancer Cell 2006;10:99–111.
12. Patil MA, Gutgemann I, Zhang J, et al. Array-based comparative genomic hybridization reveals recurrent chromosomal aberrations and Jab1 as a potential target for 8q gain in hepatocellular carcinoma. Carcinogenesis 2005;26:2050–7.
13. Midorikawa Y, Yamamoto S, Ishikawa S, et al. Molecular karyotyping of human hepatocellular carcinoma using single-nucleotide polymorphism arrays. Oncogene 2006;25:5581–90.
14. Huang J, Shen HH, Shen T, et al. Correlation between genomic DNA copy number alterations and transcriptional expression in hepatitis B virus-associated hepatocellular carcinoma. FEBS Lett 2006;580:3571–81.
15. Poon TCW, Wong N, Lai PBS, Rattray M, Johnson PJ, Sung JJY. A tumor progression model for hepatocellular carcinoma: bioinformatic analysis of genomic data. Gastroenterology 2006;131:1262–70.
16. Katoh H, Ojima H, Kokubu A, et al. Genetically distinct and clinically relevant classification of hepatocellular carcinoma: putative therapeutic targets. Gastroenterology 2007;133:1475–86.
17. Calvisi DF, Ladu S, Gorden A, et al. Mechanistic and prognostic significance of aberrant methylation in the molecular pathogenesis of human hepatocellular carcinoma. J Clin Invest 2007;117:2713–22.
18. Wurmbach E, Chen YB, Khirtrov G, et al. Genome-wide molecular profiles of HCV-induced dysplasia and hepatocellular carcinoma. Hepatology 2007;45:938–47.
19. Reich M, Liefeld T, Gould J, Lerner J, Tamayo P, Mesirov JP. GenePattern 2.0. Nat Genet 2006;38:500–1.
20. Weir BA, Woo MS, Getz G, et al. Characterizing the cancer genome in lung adenocarcinoma. Nature 2007;450:893–8.
21. Beroukhim R, Getz G, Nghiemphu L, et al. Assessing the significance of chromosomal aberrations in cancer: methodology and application to glioma. Proc Natl Acad Sci U S A 2007;104:20007–12.
22. Komura D, Shen F, Ishikawa S, et al. Genome-wide detection of human copy number variations using high-density DNA oligonucleotide arrays. Genome Res 2006;16:1575–84.
23. Llovet JM, Chen YB, Wurmbach E, et al. A molecular signature to discriminate dysplastic nodules from early hepatocellular carcinoma in HCV cirrhosis. Gastroenterology 2006;131:1758–67.
24. Irizarry RA, Bolstad BM, Collin F, Cope LM, Hobbs B, Speed TP. Summaries of Affymetrix GeneChip probe level data. Nucleic Acids Res 2003;31:e15.
25. Carter SL, Eklund AC, Mecham BH, Kohane IS, Szallasi Z. Redefinition of Affymetrix probe sets by sequence overlap with cDNA microarray probes reduces cross-platform inconsistencies in cancer-associated gene expression measurements. BMC Bioinformatics 2005;6:107.
26. Thierry-Mieg D, Thierry-Mieg J. AceView: a comprehensive cDNA-supported gene and transcripts annotation. Genome Biol 2006;7:S12.

27. Monti S, Tamayo P, Mesirov JP, Golub TR. Consensus clustering: a resampling-based method for class discovery and visualization of gene expression microarray data. Machine Learning 2003;52:91–118.

28. Tibshirani R, Hastie T, Narasimhan B, Chu G. Diagnosis of multiple cancer types by shrunken centroids of gene expression. Proc Natl Acad Sci U S A 2002;99:6567–72.

29. Llovet JM, Burroughs A, Bruix J. Hepatocellular carcinoma. Lancet 2003;362:1907–17.

30. Moinzadeh P, Breuhahn K, Stutzer H, Schirmacher P. Chromosome alterations in human hepatocellular carcinomas correlate with aetiology and histological grade—results of an explorative CGH meta-analysis. Br J Cancer 2005;92:935–41.

31. Zender L, Spector MS, Xue W, et al. Identification and validation of oncogenes in liver cancer using an integrative oncogenomic approach. Cell 2006;125:1253–67.

32. Nishida N, Fukuda Y, Komeda T, et al. Amplification and overexpression of the cyclin D1 gene in aggressive human hepatocellular carcinoma. Cancer Res 1994;54:3107–10.

33. Cadoret A, Ovejero C, Terris B, et al. New targets of β-catenin signaling in the liver are involved in the glutamine metabolism. Oncogene 2002;21:8293–301.

34. Cavard C, Terris B, Grimber G, et al. Overexpression of regenerating islet-derived 1 α and 3 α genes in human primary liver tumors with β-catenin mutations. Oncogene 2006;25:599–608.

35. Renard CA, Labalette C, Armengol C, et al. Tbx3 is a downstream target of the Wnt/β-catenin pathway and a critical mediator of β-catenin survival functions in liver cancer. Cancer Res 2007;67:901–10.

36. Whitfield ML, George LK, Grant GD, Perou CM. Common markers of proliferation. Nat Rev Cancer 2006; 6:99–106.

37. Calvisi DF, Factor VM, Ladu S, Conner EA, Thorgeirsson SS. Disruption of β-catenin pathway or genomic instability define two distinct categories of liver cancer in transgenic mice. Gastroenterology 2004; 126:1374–86.

38. Taylor MW, Tsukahara T, Brodsky L, et al. Changes in gene expression during pegylated interferon and ribavirin therapy of chronic hepatitis C virus distinguish responders from nonresponders to antiviral therapy. J Virol 2007;81:3391–401.

39. Asselah T, Bieche I, Narguet S, et al. Liver gene expression signature to predict response to pegylated interferon plus ribavirin combination therapy in patients with chronic hepatitis C. Gut 2008;57:516–24.

40. Llovet JM, Bruix J. Molecular targeted therapies in hepatocellular carcinoma. Hepatology. In press, 2008.

41. Okamoto H, Yasui K, Zhao C, Arii S, Inazawa A. PTK2 and EIF3S3 genes may be amplification targets at 8q23-24 and are associated with large hepatocellular carcinomas. Hepatology 2003;38:1242–9.

42. Lee JS, Chu IS, Mikaelyan A, et al. Application of comparative functional genomics to identify best-fit mouse models to study human cancer. Nat Genet 2004; 36:1306–11.

43. Chen YJ, Yeh SH, Chen JT, et al. Chromosomal changes and clonality relationship between primary and recurrent hepatocellular carcinoma. Gastroenterology 2000;119:431–40.

44. Mise M, Arii S, Higashituji H, et al. Clinical significance of vascular endothelial growth factor and basic fibroblast growth factor gene expression in liver tumors. Hepatology 1996;23:455–64.

45. Poon RT, Ho JW, Tong CS, Lau C, Ng IO, Fan ST. Prognostic significance of serum vascular endothelial growth factor and endostatin in patients with hepatocellular carcinoma. Br J Surg 2004;91:1354–60.

46. Wilhelm SM, Carter C, Tang LY, et al. BAY 43-9006 exhibits broad spectrum oral antitumor activity and targets the RAF/MEK/ERK pathway and receptor tyrosine kinases involved in tumor progression and angiogenesis. Cancer Res 2004;64:7099–109.

47. Llovet JM, Ricci S, Mazzaferro V, et al. Sorafenib in advanced hepatocellular cancer. N Engl J Med 2008;359: 378–90.

48. Shimizu H, Miyazaki M, Wakabayashi Y, et al. Vascular endothelial growth factor secreted by replicating hepatocytes induces sinusoidal endothelial cell proliferation during regeneration after partial hepatectomy in rats. J Hepatol 2001;34:683–9.

49. LeCouter J, Moritz DR, Li B, et al. Angiogenesis-independent endothelial protection of liver: role of VEGFR-1. Science 2003;299:890–3.

50. Hao JH, Yu M, Li HK, Shi YR, Li Q, Hao XS. Inhibitory effect of antisense vascular endothelial growth factor RNA on the profile of hepatocellular carcinoma cell line *in vitro* and *in vivo*. World J Gastroenterol 2006;12:1140–3.